



## Iron(III) aroylhydrazone complexes: Structure, electrochemical studies and catalytic activity in oxidation of olefins

Hassan Hosseini Monfared<sup>a,\*</sup>, Somayeh Sadighian<sup>a</sup>, Mohammad-Ali Kamyabi<sup>a</sup>, Peter Mayer<sup>b</sup>

<sup>a</sup> Department of Chemistry, Zanjan University 45195-313, Zanjan, Islamic Republic of Iran

<sup>b</sup> Fakultät für Chemie und Pharmazie, Ludwig-Maximilians-Universität, München, Butenandtstr. 5-13, Haus D, D-81377 München, Germany

### ARTICLE INFO

#### Article history:

Received 16 December 2008

Received in revised form 3 February 2009

Accepted 3 February 2009

Available online 13 February 2009

#### Keywords:

Crystal structure

Aroylhydrazone

Olefins

Epoxidation

Iron catalyst

Cyclic voltammetry

### ABSTRACT

Tridentate Schiff base ligands derived from aromatic aldehydes and benzhydrazide, and their iron complexes  $[\text{Fe}(\text{L}^1)(\text{HL}^1)]$  **1**,  $[\text{Fe}(\text{HL}^1)\text{Cl}_2(\text{CH}_3\text{OH})\cdot(\text{CH}_3\text{OH})]$  **2** and  $[\text{Fe}(\text{HL}^2)\text{Cl}_2(\text{H}_2\text{O})]$  **3** have been prepared and characterized ( $\text{H}_2\text{L}^1 = (E)\text{-N}'\text{-(2-hydroxy-3-methoxybenzylidene)benzohydrazide}$ ,  $\text{H}_2\text{L}^2 = (E)\text{-N}'\text{-(5-bromo-2-hydroxybenzylidene)benzohydrazide}$ ). The crystal structure of **2** has been determined. The electrochemical properties of these complexes have been investigated by cyclic voltammetric technique in acetonitrile solutions. Electrochemical studies have revealed quasi-reversibility for these compounds. The catalytic potential of these complexes has been tested for the oxidation of cyclooctene using *tert*-butylhydroperoxide (TBHP) as oxidant. The effects of the molar ratio of oxidant to substrate, the temperature, the co-catalyst concentration and the solvent have been studied. Excellent selectivities have been obtained for the epoxidation of cyclohexene, cyclooctene, norbornene, *cis*- and *trans*-stilbene.

© 2009 Elsevier B.V. All rights reserved.

### 1. Introduction

The design of metal catalysts to mimic bio-oxidative activity of P-450 has continued to be an active area of research [1]. There have been numerous reports on the catalytic oxidation of organic substrates by porphyrin complexes [2,3]. Due to the difficulties in modification, the preparation of other planar tetradentate ligands, especially Schiff base [4,5] and amido ligands [6], is highly desirable. The oxidation of hydrocarbons with Schiff base complexes has been a field of academic and industrial interest to analyze the catalytic activity of various metal complexes [7]. Schiff bases play an important role in inorganic chemistry as they easily form stable complexes with most transition metal ions. The development in the field of bioinorganic chemistry has increased the interest in Schiff base complexes, since it has been recognized that many of these complexes may serve as models for biologically important species [8]. Iron-catalyzed systems for C–H oxidation (Gif8 and Fenton chemistry [9], nonheme mimic systems [10–12], olefin epoxidation [5], and the chemistry of Fe-porphyrins [13]) have been summarized in various reports.

The remarkable biological activity of acid hydrazides  $\text{R-CO-NH-NH}_2$ , a class of Schiff base, their corresponding

aroylhydrazones,  $\text{R-CO-NH-N=CH-R}'$ , and the dependence of their mode of chelation with transition metal ions present in the living system have been of significant interest [14–17]. The coordination compounds of aroylhydrazones have been reported to act as enzyme inhibitors [18] and are useful due to their pharmacological applications [19]. Aroylhydrazones complexes, on the other hand, seem to be a good candidate for catalytic oxidation studies because of their stability to resist oxidation. Investigation into the iron-binding potential of a range of hydrazone derivatives [20–22], as drugs for genetic disorders such as thalassemia, led to the discovery that salicylaldehyde benzoylhydrazone inhibits DNA synthesis and cell growth [23]. This class of diprotic ligand typically acts as tridentate, planar chelate ligand coordinating through the phenolic and amide oxygens and the imine nitrogen. The actual ionization state is dependent upon the conditions and metal employed [24]. With copper(II) in alkaline solution, both the phenolic and amide protons are ionized; in neutral and mild acidic solution the ligands are monoanionic, whereas strongly acidic conditions are necessary to form compounds formulated with a neutral ligand. A binuclear complex of iron(III) with a Schiff base hydrazone derived from 7-chloro-4-hydrazinoquinoline and bridging chloride has been reported [25].

Continuing our studies on catalysis by hydrazone Schiff base manganese complexes [26], we report herein on the synthesis of a series of iron(III) complexes containing substituted aroylhydrazones ligands (Fig. 1) as well as their applications in catalytic epoxidation of olefins with *tert*-butylhydroperoxide.

\* Corresponding author. Tel.: +98 241 5152576; fax: +98 241 2283203.

E-mail addresses: [monfared@znu.ac.ir](mailto:monfared@znu.ac.ir), [monfared.2@yahoo.com](mailto:monfared.2@yahoo.com) (H.H. Monfared).

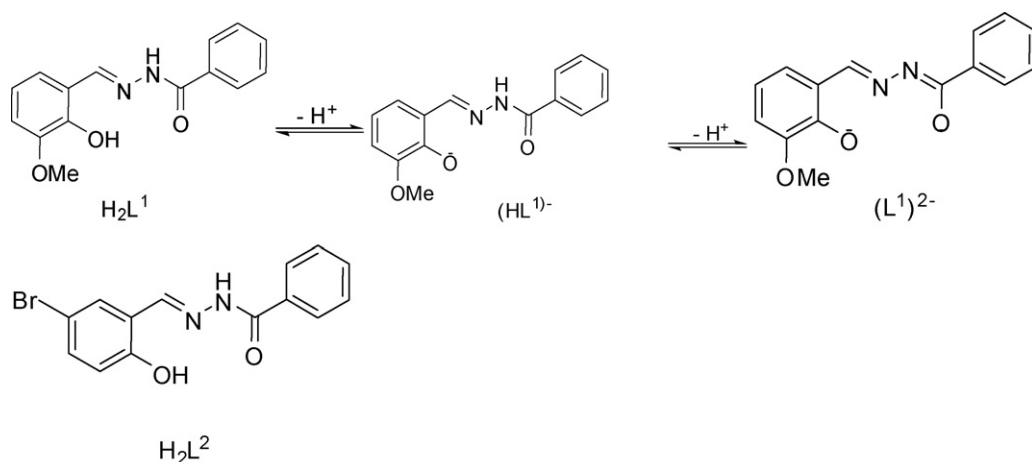


Fig. 1. *In situ* formed  $\text{H}_2\text{L}^1$  and  $\text{H}_2\text{L}^2$  ligands.

## 2. Experimental

### 2.1. Equipments

The reaction products of oxidation were determined and analyzed by HP Agilent 6890 gas chromatograph equipped with a HP-5 capillary column (phenyl methyl siloxane  $30\text{ m} \times 320\ \mu\text{m} \times 0.25\ \mu\text{m}$ ) with flame-ionization detector and gas chromatograph–mass spectrometry (Hewlett-Packard 5973 Series MS-HP gas chromatograph with a mass-selective detector).  $^1\text{H}$  NMR spectra were recorded by use of a Bruker 250 MHz spectrometer. Atomic absorptions were measured by a Varian 220 FS spectrophotometer. Microanalyses were carried out using a Heraeus CHN-O– Rapid analyzer. IR spectra were recorded using PerkinElmer 597 and Nicolet 510P spectrophotometers. A Thermospectronic model  $\alpha$ , UV–vis spectrometer with 1 cm quartz cells was used for recording and storage of UV–vis absorbance spectra.

### 2.2. Experimental

Voltammetric experiments were performed using a Metrohm computrace voltammetric analyzer model 757 VA. A conventional three-electrode system was used with a polished glassy carbon electrode (area  $3.14\ \text{mm}^2$ ) as working electrode and a platinum wire counter electrode. The reference was an aqueous Ag/AgCl saturated electrode, separated from the bulk of the solution by a bridge with solvent and supporting electrolyte. The solutions in the bridge were changed periodically to avoid aqueous contamination from entering the cell via the Ag/AgCl electrode. Before each experiment the working electrode was cleaned by polishing with alumina 0.05 mm and rinsed thoroughly with distilled water and acetone. The electrolytic medium consisted of 0.1 mol/l tetrabutylammonium perchlorate (TBAP) as supporting electrolyte in acetonitrile and all experiments were carried out at room temperature. The solutions were freshly prepared before use, and were purged with  $\text{N}_2$  saturated with solvent for ca. 15 min prior to taking measurements in order to remove dissolved  $\text{O}_2$ . Voltammograms were recorded in the range from  $-0.7$  to  $+0.7\ \text{V}$  vs. Ag/AgCl.

### 2.3. Materials

Iron(III) chloride hexahydrate, anhydrous iron(II) chloride, benzhydrazide, 2-hydroxy-3-methoxybenzaldehyde, 5-bromo-2-

hydroxybenzaldehyde, *tert*-butylhydroperoxide (TBHP) (solution 80% in di-*tert*-butylperoxide) and the olefins were purchased from Merck and Fluka and used as received. Solvents of the highest grade commercially available (Merck) were used without further purification.

### 2.4. Synthesis of $[\text{Fe}^{\text{III}}(\text{L}^1)(\text{HL}^1)]$ , **1** ( $\text{H}_2\text{L}^1 = (E)\text{-}N'\text{-(2-hydroxy-3-methoxybenzylidene)benzohydrazide}$ )

Benzhydrazide (0.20 g, 1.47 mmol) and 2-hydroxy-3-methoxybenzaldehyde (0.22 g, 1.47 mmol) were dissolved in methanol (100 ml). A solution of  $\text{FeCl}_3 \cdot 6\text{H}_2\text{O}$  (0.40 g, 0.148 mmol) and  $\text{NaN}_3$  (0.147 g, 2.26 mmol) in methanol (50 ml) was added to the above solution and refluxed for 3 h. The resulting black-brown solid **1** was filtered off, washed with methanol and dried under air (0.319 g, yield 73%).

IR (KBr,  $\text{cm}^{-1}$ ): 3371 (s), 3170 (s, br), 2785 (w), 1682 (vs), 1620 (s, br), 1396 (s), 1365 (m), 1203 (m), 1026 (m), 779 (m), 702 (m), 609 (s), 509 (m), 409 (m).

### 2.5. Synthesis of $[\text{Fe}(\text{HL}^1)\text{Cl}_2(\text{CH}_3\text{OH})] \cdot \text{CH}_3\text{OH}$ , **2**

Benzhydrazide (0.20 g, 1.47 mmol) and 2-hydroxy-3-methoxybenzaldehyde (0.22 g, 1.47 mmol) were dissolved in methanol (100 ml). A solution of  $\text{FeCl}_3 \cdot 6\text{H}_2\text{O}$  (0.40 g, 1.48 mmol) in methanol (50 ml) was added to the above solution and refluxed for 3 h. The resulting black-green solid **2** was filtered off, washed with methanol and dried under air (0.636 g, yield 94%).

IR (KBr,  $\text{cm}^{-1}$ ): 3431 (vs, br), 3231 (s), 2931 (m), 2862 (w), 1600 (vs), 1546 (vs), 1438 (s), 1392 (s), 1315 (m), 1262 (m), 1223 (s), 1092 (s), 746 (w), 708 (m).

### 2.6. Synthesis of $[\text{Fe}(\text{HL}^2)\text{Cl}_2(\text{H}_2\text{O})]$ , **3** ( $\text{H}_2\text{L}^2 = (E)\text{-}N'\text{-(5-bromo-2-hydroxybenzylidene)benzohydrazide}$ )

Benzhydrazide (0.20 g, 1.47 mmol) and 5-bromo-2-hydroxybenzaldehyde (0.30 g, 1.49 mmol) were dissolved in methanol (100 ml). A solution of  $\text{FeCl}_3 \cdot 6\text{H}_2\text{O}$  (0.40 g, 1.48 mmol) in methanol (50 ml) was added to the above solution and refluxed for 3 h. The resulting black-brown solid **2** was filtered off, washed with methanol and dried under air (0.480 g, yield 69%).

IR (KBr,  $\text{cm}^{-1}$ ): 3431 (s, br), 3215 (m), 2923 (m), 2862 (w), 1608 (vs), 1562 (m), 1531 (m), 1500 (m), 1462 (s), 1374 (s), 1346 (m), 1300 (s), 1185 (vs, br), 1092 (s), 715 (m), 654 (m), 600 (m).

**Table 1**  
Crystallographic data of **2**.

Net formula	C <sub>17</sub> H <sub>21</sub> Cl <sub>2</sub> FeN <sub>2</sub> O <sub>5</sub> ·(CH <sub>3</sub> OH)
M <sub>r</sub> (g mol <sup>-1</sup> )	460.110
T (K)	200(2)
Crystal system	Monoclinic
Space group	P2 <sub>1</sub> /c
a (Å)	18.8683(6)
b (Å)	9.0534(5)
c (Å)	12.0460(5)
α (°)	90
β (°)	107.673(3)
γ (°)	90
V (Å <sup>3</sup> )	1960.61(15)
Z	4
Calc. density (g cm <sup>-3</sup> )	1.55878(12)
μ (mm <sup>-1</sup> )	1.072
Absorption correction	None
Refls. measured	11947
R <sub>int</sub>	0.0507
Mean σ(I)/I	0.0448
θ range	3.19–25.25
Observed refls.	2779
x, y (weighting scheme)	0.0529, 19.3334
Hydrogen refinement	Mixed
Refls. in refinement	3534
Parameters	257
Restraints	3
R(F <sub>obs</sub> )	0.0710
R <sub>w</sub> (F <sup>2</sup> )	0.2048
S	1.132
Shift/error <sub>max</sub>	0.001
Max electron density/e (Å <sup>-3</sup> )	0.700
Min electron density/e (Å <sup>-3</sup> )	-0.622

**Table 2**  
IR spectral data of the ligands and the iron complexes.

Compound	Selected IR bands (cm <sup>-1</sup> )			
	$\bar{\nu}(\text{C}=\text{N}) + \delta(\text{NH})$	$\bar{\nu}(\text{C}=\text{O})$	$\bar{\nu}(\text{NH})$	$\bar{\nu}(\text{OH})$
H <sub>2</sub> L <sup>1</sup>	1607, 1577	1653	3215	3569, 3376
H <sub>2</sub> L <sup>2</sup>	1615, 1546	1646	3215	3415
<b>1</b>	1620	1682	3170	3371
<b>2</b>	1546	1600	3231	3431(broad)
<b>3</b>	1562, 1531	1608	3215	3431 (broad)

### 2.7. X-ray crystallography

A dark green crystal of **2** (0.01 mm × 0.08 mm × 0.16 mm) was investigated in a diffraction experiment at 200(2)K on a Nonius Kappa CCD diffractometer with monochromated Mo Kα radiation (λ = 0.71073) obtained from a graded multilayer X-ray optics. The structure was solved by Direct Methods with SIR97 [27], and refined with full-matrix least-squares techniques on F<sup>2</sup> with SHELXL-97 [28]. The crystal data and refinement parameters are presented in Table 1. The C-bonded hydrogen atoms were calculated in idealized geometry riding on their parent atoms. The O- and N-

bonded hydrogen atoms were located from the difference map with U(H) = 1.5 × U<sub>iso</sub>(O) and U(H) = 1.2U<sub>iso</sub>(N). The molecular structure plot was prepared using ORTEPIII [29].

CCDC 711373 contains the supplementary crystallographic data for **2**. These data can be obtained free of charge from The Cambridge Crystallographic Data Centre via [www.ccdc.cam.ac.uk/data\\_request/cif](http://www.ccdc.cam.ac.uk/data_request/cif).

### 2.8. General oxidation procedure

Oxidation reactions were performed in a stirred round-bottom flask fitted with a water-cooled condenser. The reactions were carried out under atmospheric pressure in air in an oil bath at 60 ± 1 °C with acetonitrile as a solvent and TBHP as an oxidant. In a typical experiment a mixture of 0.0022 mmol catalyst, 5.0 ml solvent, 1.0 mmol olefin, 0.073 mmol imidazole, and 1.0 mmol *n*-octane as internal standard was prepared in a round-bottom flask. After the mixture was heated to 60 °C, 2.0 mmol TBHP was added. At appropriate intervals, aliquots were removed and analyzed immediately by GC. Oxidation products yields based on the starting substrate were quantified by comparison with *n*-octane.

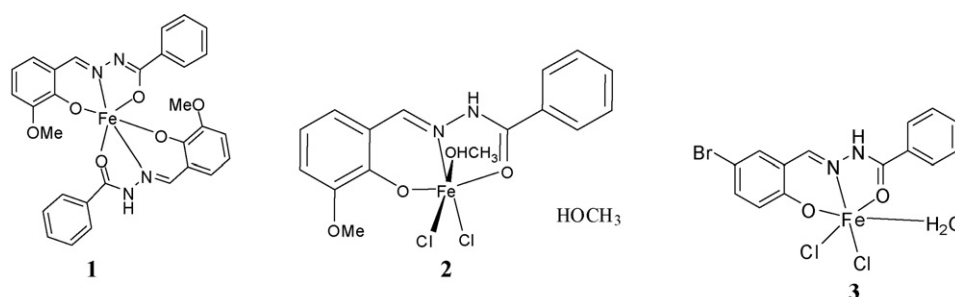
## 3. Results and discussion

### 3.1. Characterization of the Fe(III) complexes

The H<sub>2</sub>L<sup>1</sup> and H<sub>2</sub>L<sup>2</sup> are formed *in situ* when equimolar quantities of 2-hydroxy-3-methoxybenzaldehyde or 5-bromo-2-hydroxybenzaldehyde and benzohydrazide are reacted with iron chloride in methanol, respectively [30]. The *in situ* formed ligand could be in equilibrium with mono-(HL)<sup>-</sup> and dianionic (L)<sup>2-</sup> forms (Fig. 1). Depending on the reaction conditions, H<sub>2</sub>L may coordinate to a metal center as a monoanionic (HL)<sup>-</sup> [26] or a dianionic (L)<sup>2-</sup> ligand [31]. The pK<sub>a1</sub> and pK<sub>a2</sub> values obtained for the acidity constants of H<sub>2</sub>L<sup>1</sup> are 9.03 and 10.92, respectively [32]. So, under neutral or less basic conditions of FeCl<sub>3</sub>·6H<sub>2</sub>O in methanol, H<sub>2</sub>L acts as a monoanionic tridentate chelating ligand by phenolic oxygen deprotonation.

A practical list of IR spectral data is presented in Table 2. A comparison of the spectra of the complexes with the ligands provides evidence for the coordination mode of the ligands in the catalysts. The hydrazone Schiff base ligand (H<sub>2</sub>L<sup>1</sup>) exhibits three bands on 3215–3569 cm<sup>-1</sup> due to phenolic and -NH-vibrations. The presence of a NH band, red shifts in azomethine (-C=N-, 61 cm<sup>-1</sup>) and carbonyl bands (53 cm<sup>-1</sup>) of the H<sub>2</sub>L<sup>1</sup> ligand indicate coordination of H<sub>2</sub>L<sup>1</sup> through the deprotonated hydroxyl group, azomethine nitrogen and amide oxygen groups in the complex **2** (Table 2). The analytical and physical data of the complexes are given in Table 3. Suggested structures of complexes **1** and **3** could be rationalized in the same way (Fig. 2).

Caused by complexation, the UV-vis spectra of **1**, **2** and **3** in methanol show absorbance bands at 362, 305, 233 for complex

**Fig. 2.** Proposed structures of octahedral geometry of **1**, **2**, and **3**.

**Table 3**  
Analytical and physical data of the complexes.

Empirical formula	Formula weight (g mol <sup>-1</sup> )	Yield (%)	Color	Analyses found (calc.) (%)			
				%C	%H	%N	%Fe
<b>1</b> , C <sub>30</sub> H <sub>25</sub> FeN <sub>4</sub> O <sub>6</sub>	593.39	74	Black-brown	60.50 (60.72)	4.50 (4.25)	9.40 (9.44)	10.00 (9.41)
<b>2</b> , C <sub>17</sub> H <sub>21</sub> Cl <sub>2</sub> FeN <sub>2</sub> O <sub>5</sub>	460.11	94	Black-green	44.00 (44.38)	4.55 (4.60)	6.00 (6.09)	12.11 (12.14)
<b>3</b> , C <sub>14</sub> H <sub>12</sub> BrCl <sub>2</sub> FeN <sub>2</sub> O <sub>3</sub>	462.91	69	Black-brown	36.2 (36.32)	2.60 (2.61)	6.30 (6.05)	12.25 (12.06)

**1**, at 304, 226 for complex **2**, and at 362, 292, 227 for complex **3**, slightly different from those at 338, 262, 222 of the corresponding free ligand H<sub>2</sub>L<sup>1</sup> (all absorbances are given in nm).

### 3.2. X-ray structure of [Fe(HL<sup>1</sup>)Cl<sub>2</sub>(CH<sub>3</sub>OH)]·(CH<sub>3</sub>OH), **2**

The X-ray study reveals that **2** crystallizes in the monoclinic space group *P*2<sub>1</sub>/*c* with four formula units in the unit cell. The molecular structure of the complex and the labelling of the atoms are shown in Fig. 3. Crystallographic data and structure refinement parameters are given in Table 3. The Fe(III) atom is meridionally coordinated by O, N, O donor set of the (*E*)-*N'*-(2-hydroxy-3-methoxybenzylidene)benzohydrazide ligand. Two *cis*-coordinated chloro and a methanol ligand complete the distorted pseudo-octahedral metal coordination sphere. The metal center in **2** is displaced by 0.143 Å out of the least-squares plane defined by the donor atoms O2, N2, Cl2 and O1.

Adjacent molecules of **2** are connected together by strong hydrogen bonds N1–H71..O2 and N1–H71..O3 which leads to an infinite 1-D chain along [001] (Fig. 4, Table 4).

### 3.3. Electrochemical studies

Cyclic voltammograms (CVs) of the complexes **1–3** were recorded in acetonitrile with TBAP as supporting electrolyte in the

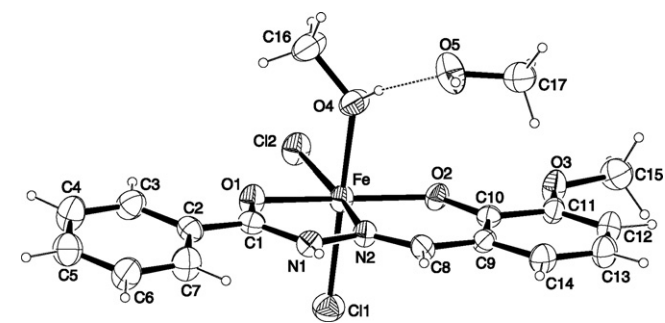
potential range –0.7 to +0.7 V vs. Ag/AgCl. Typical CVs of **1–3** are shown in Fig. 5. The redox parameters from CVs of **1** and **2** are nearly identical with  $E^0 = +0.049$  V (vs. Ag/AgCl), which can be ascribed to the redox reaction Fe<sup>III</sup>/Fe<sup>II</sup>. However, complex **3** shows a very weak redox peak at the same condition. The cyclic voltammogram of the complex **2** in acetonitrile displays a quasi-reversible peak at  $E^0 = +0.049$  V (vs. Ag/AgCl). The  $\Delta E_p = (E_{pa} - E_{pc})$  value was 125 mV and the  $i_{pa}/i_{pc} = 0.6$ . This finding shows a quasi-reversibility of this redox process. Electrochemical studies have also revealed quasi-reversibility for **1** and **3**.

The cyclic voltammograms of complex **2** at different scan rates from 10 to 1000 mV s<sup>-1</sup> are illustrated in Fig. 6. Obviously the sep-

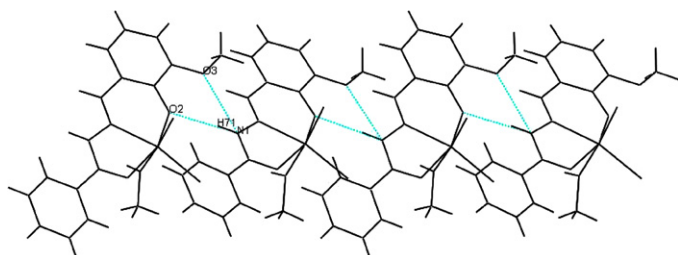
**Table 4**  
Hydrogen bonding interactions for **2**.

D–H...A	D–H (Å)	H...A (Å)	D...A (Å)	D–H...A (°)
N1–H71...O2 <sup>a</sup>	0.879(18)	2.16(3)	3.022(7)	165(7)
N1–H71...O3 <sup>a</sup>	0.879(18)	2.39(7)	2.941(8)	121(6)

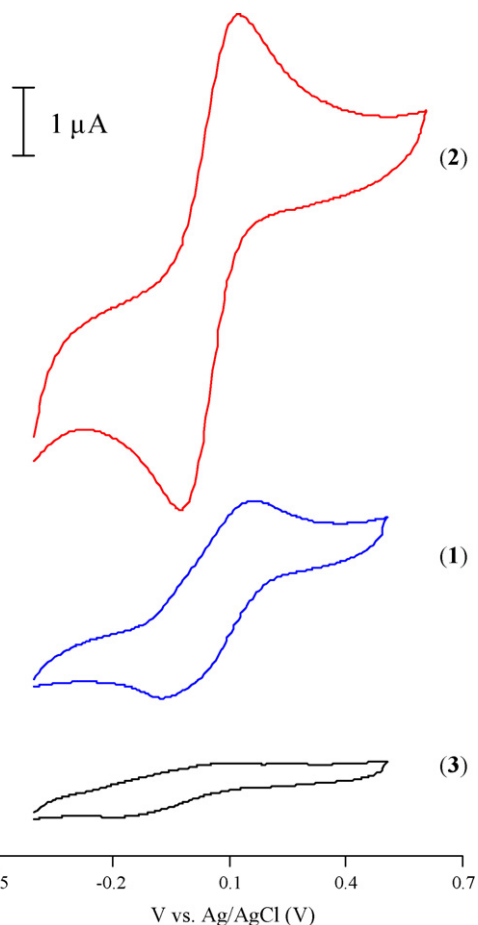
<sup>a</sup> Symmetry transformation:  $x, 1/2 - y, -1/2 + z$ .



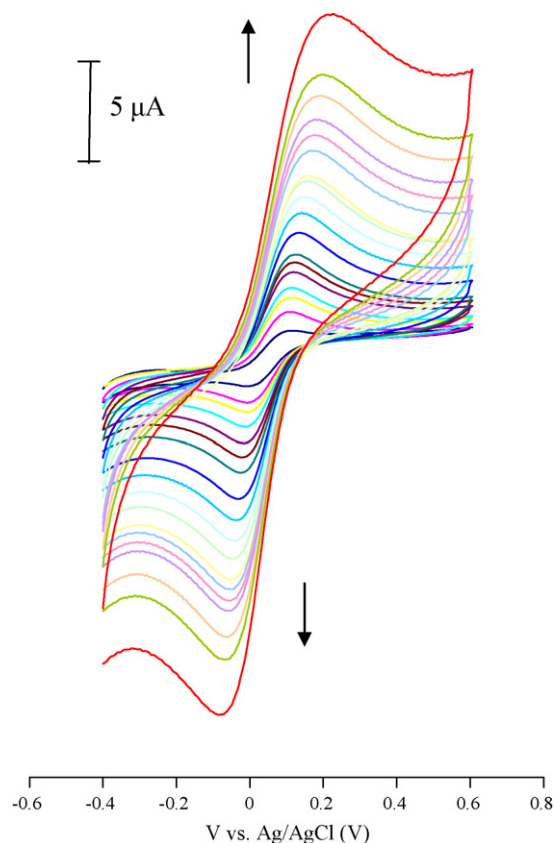
**Fig. 3.** The molecular structure of **2**. Ellipsoids are drawn at the 50% probability level. Selected distances (Å) and angles (°): Fe–Cl1 2.320(2), Fe–Cl2 2.2610(19), Fe–O1 2.077(6), Fe–O2 1.935(4), Fe–O4 2.104(6), Fe–N2 2.130(6) Cl1–Fe–Cl2 96.06(8), Cl1–Fe–O1 93.10(17), Cl1–Fe–O2 94.74(14), Cl1–Fe–O4 175.93(17), Cl1–Fe–N2 90.75(16), Cl2–Fe–O1 93.64(15), Cl2–Fe–O2 105.90(15), Cl2–Fe–O4 87.84(17), Cl2–Fe–N2 166.15(17), O1–Fe–O2 158.0(2), O1–Fe–O4 85.5(2), O1–Fe–N2 73.9(2), O2–Fe–O4 85.3(2), O2–Fe–N2 85.5(2), O4–Fe–N2 85.2(2).



**Fig. 4.** One-dimensional chain along [001] formed by intermolecular hydrogen bonds (viewing direction along [010]).



**Fig. 5.** Cyclic voltammogram of **1**, **2** and **3** (10<sup>-3</sup> mol/l) in acetonitrile and TBAP (0.1 mol/l); scan rate 100 mV s<sup>-1</sup>.



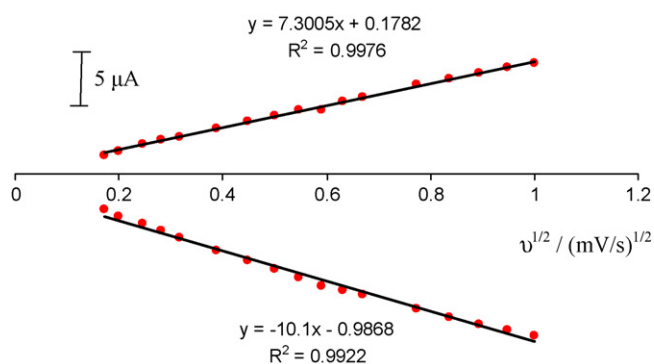
**Fig. 6.** Cyclic voltammogram of **2** ( $10^{-3}$  mol/l) in acetonitrile and TBAP (0.1 mol/l); scan rate 10, 20, 30, 40, 60, 80, 100, 150, 200, 250, 300, 350, 400, 450, 500, 600, 700, 800, 900 and 1000  $\text{mV s}^{-1}$ .

aration between  $E_p$  increases as the scan rate increases and this is characteristic of a quasi-reversible system. There is a linear relationship between the cathodic and anodic peak currents and the square root of the scan rate ( $\nu^{1/2}$ ) in the 10–1000  $\text{mV s}^{-1}$  range (Fig. 7). This behavior is typical for an electron transfer process controlled by diffusion.

### 3.4. Catalytic activity studies

#### 3.4.1. Oxidation of cyclooctene

The oxidation of cyclooctene catalyzed by **1**, **2**, and **3** was carried out with *tert*-butylhydroperoxide as an oxidant to give cyclooctene oxide as the sole product. The results of control experiments revealed that the presence of catalyst and oxidant are essential for the oxidation. The oxidation of cyclooctene in the absence of TBHP



**Fig. 7.** Plot of cathodic and anodic currents vs. the square root of sweep rate ( $\nu^{1/2}$ ) for **2**.

**Table 5**

Control experiments for catalytic oxidation of cyclooctene.

No.	Catalyst	Co-catalyst	Oxidant	%Conversion	Time (h)
1	<b>2</b>	Imidazole	None	0 (0)	4 (24)
2	None	Imidazole	TBHP	0 (6)	4 (24)
3	<b>2</b>	None	TBHP	14 (19)	4 (24)
4	<b>2</b>	Imidazole	TBHP	55 (70)	4 (24)

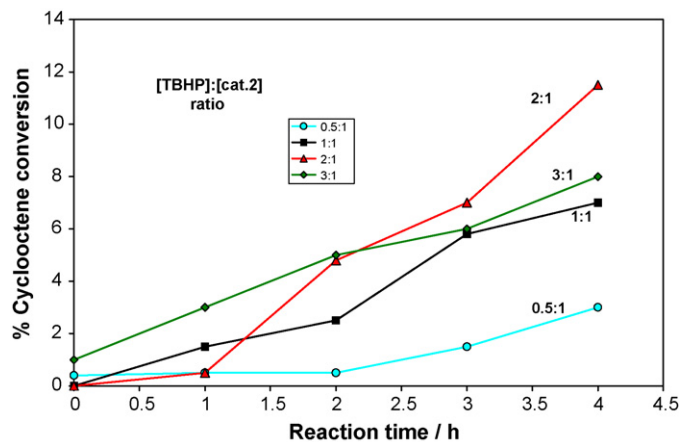
Reaction conditions: cyclooctene (1.0 mmol), TBHP (2.0 mmol), catalyst **2** (0.0022 mmol), acetonitrile (5 ml), imidazole (0.073 mmol) and temperature ( $60 \pm 1^\circ\text{C}$ ).

does not occur (Table 5, no. 1) and in the absence of catalyst the oxidation proceeds only up to 6% after 24 h (Table 5, no. 2). Addition of a co-catalyst (imidazole) increases the cyclooctene conversion from 19 to 70% (Table 5, no. 3 and 4).

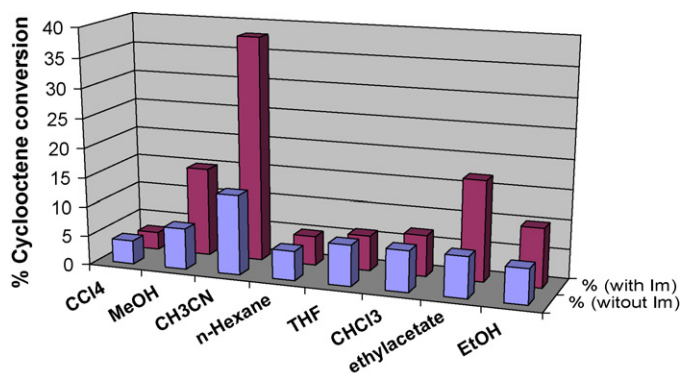
In search of suitable reaction conditions to achieve the maximum oxidation of cyclooctene, the effect of oxidant concentration (moles of TBHP per moles of cyclooctene), solvent and temperature of the reaction were studied. The effect of TBHP concentration on the oxidation of cyclooctene is illustrated in Fig. 8. Different TBHP/cyclooctene molar ratios (0.5:1, 1:1, 2:1 and 3:1) were considered while keeping the fixed amount of cyclooctene (1.0 mmol) and catalyst **2** (0.0022 mmol) in 5 ml of ethylacetate at  $60 \pm 1^\circ\text{C}$ . Increasing the TBHP/cyclooctene ratio from 0.5:1 to 2:1 increases the conversion from 3 to 11%. Further increment results to reduction of conversion. The maximum cyclooctene conversion is obtained with a molar ratio of 2:1.

Fig. 9 illustrates the influence of the solvent nature in the catalytic epoxidation of cyclooctene by **2**. Carbon tetrachloride, methanol, ethanol, acetonitrile, chloroform, *n*-hexane, tetrahydrofuran (THF) and ethyl acetate were used as solvents. The highest conversion was obtained in acetonitrile, 14% in the absence of imidazole and 38% in the presence of imidazole. It was observed that the catalytic activity of the complex **2** decreases in order acetonitrile > ethyl acetate > methanol > ethanol > chloroform > tetrahydrofuran > *n*-hexane > carbon tetrachloride at a temperature of  $60 \pm 1^\circ\text{C}$ . The highest conversion in acetonitrile possibly is caused by its dielectric constant ( $\epsilon/\epsilon_0 = 35.94$ ) and dipole moment ( $\mu = 3.90\text{D}$ ) which are the highest of all the solvents used.

In order to get the best reaction temperature, the reaction mixture was stirred at various temperatures (for results see Fig. 10). With **2** as catalyst a maximum conversion of cyclooctene (55%) is obtained after 4 h at  $60^\circ\text{C}$ . A temperature rise up to  $80^\circ\text{C}$  lowers the cyclooctene conversion. The highest conversion of cyclooctene



**Fig. 8.** Effect of TBHP concentration on oxidation of cyclooctene by **2**. Reaction conditions: cyclooctene (1.0 mmol), *n*-octane (1.0 mmol), catalyst (0.0022 mmol), imidazole (0.10 mmol), ethylacetate (5.0 ml) and temperature ( $60 \pm 1^\circ\text{C}$ ).



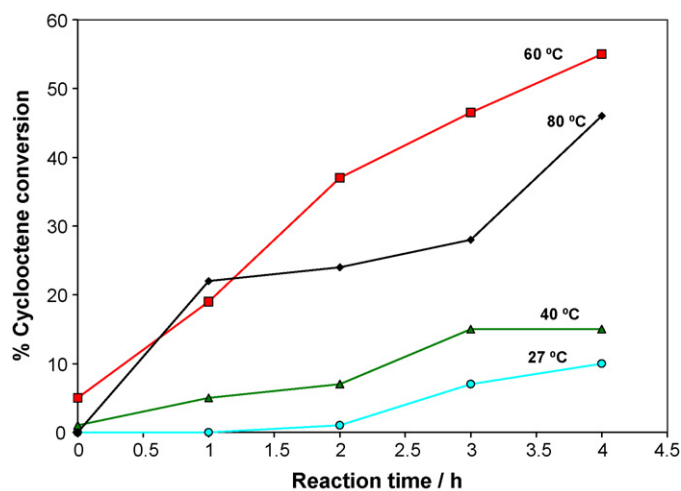
**Fig. 9.** Effect of solvent on oxidation of cyclooctene by **2**. Reaction conditions: cyclooctene (1.0 mmol), *n*-octane (1.0 mmol), catalyst (0.0022 mmol), imidazole (0.10 mmol), solvent (5.0 mmol), TBHP (2.0 mmol), reaction times (4 h) and temperature ( $60 \pm 1$  °C) in the absence imidazole and presence of imidazole (0.10 mmol).

was also obtained at 60 °C when the reaction continued until 24 h.

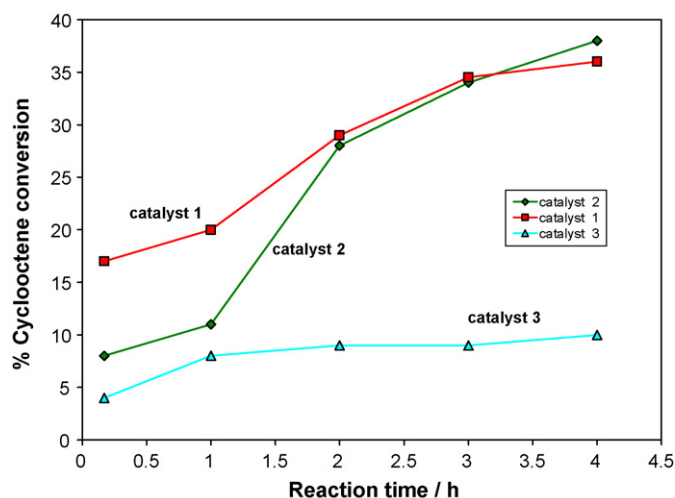
In addition to the catalyst, the presence of a nitrogenous base like imidazole as a co-catalyst increased the conversion of cyclooctene. It is well established that imidazole has more influence than pyridine as a fifth ligand in heme compounds [33]. It has been suggested that, in addition to  $\pi$  basicity (sideways basicity), unusually large  $\pi$  basicity of imidazole compared to other  $\pi$  bases leads to a stronger iron back-bond with the empty electronegative  $\pi^*$  orbitals of oxygen [33].

The catalytic activities of **1**, **2**, and **3** were examined under the optimized conditions for catalyst **2** (TBHP/cyclooctene ratio = 2, acetonitrile, reaction temperature 60 °C). Catalyst **3** shows the lowest (10%) and catalyst **2** shows the highest activity (38%) in the oxidation of cyclooctene with TBHP (Fig. 11).

The effect of the imidazole concentration on the oxidation of cyclooctene is illustrated in Fig. 12. Different imidazole/catalyst molar ratios (7:1, 33:1, 45:1 and 68:1) were considered while keeping the fixed amount of cyclooctene (1 mmol) and catalyst **2** (0.0022 mmol) in 5 ml of acetonitrile at  $60 \pm 1$  °C. Increasing the imidazole/catalyst ratio from 7:1 to 33:1 increases the conversion from 19 to 55%. A higher ratio reduces the conversion. The maximum cyclooctene conversion is obtained with a molar ratio of 33:1.



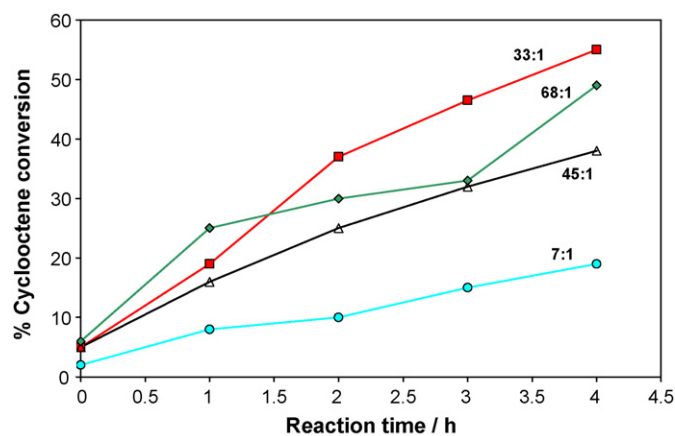
**Fig. 10.** Effect of temperature on conversion of cyclooctene by **2**. Reaction conditions: cyclooctene (1.0 mmol), *n*-octane (1.0 mmol), catalyst (0.0022 mmol), imidazole (0.073 mmol), acetonitrile (5.0 mmol) and TBHP (2.0 mmol).



**Fig. 11.** Effects of the catalyst nature on the oxidation of cyclooctene. Reaction conditions: cyclooctene (1.0 mmol), *n*-octane (1.0 mmol), catalyst (0.0022 mmol), imidazole (0.10 mmol), acetonitrile (5.0 ml), TBHP (2.0 mmol), and temperature ( $60 \pm 1$  °C).

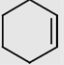
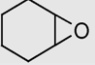

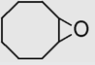


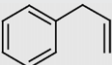
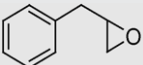
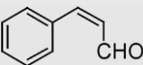
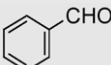


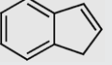
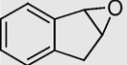
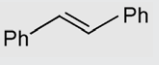
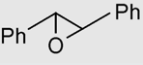
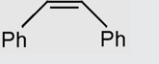
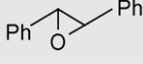
### 3.4.2. Oxidation of various olefins

Finally, in order to explore further the oxidation potential of the hydrazone Schiff base catalyst **2**, oxidation of various olefins was performed under the same reaction conditions which proved to be the best for cyclooctene. We have studied linear, cyclic and phenyl substituted olefins as substrates. Epoxidation of various olefins by TBHP in the presence of **2** and imidazole proceeded quantitatively in  $\text{CH}_3\text{CN}$ . This catalytic system led to the epoxidation of various olefins (Table 6) with good conversions (31–80%) (except for indene with 9% conversion) and excellent epoxide selectivity. The only exception was the oxidation of allyl benzene, where 8% 3-phenyl-propenal, 5% benzaldehyde and 60% 2-benzyl-oxirane were obtained (Table 6). Electron-rich cyclohexene and cyclooctene displayed a greater reactivity than terminal olefins. The relatively electron-poor 1,3-cyclooctadiene shows lower reactivity than cyclooctene. This reflects the electrophilic nature of the oxygen transfer from the plausible iron–oxo intermediate to the olefinic double bond. Allylic oxidation or formation of by-products, which is seen in the metalloporphyrin systems [34,35] was not observed in the epoxidation of alkenes such as cyclohexene. The higher reactivity of cyclohexene relative to cyclooctene might be due to the greater angle strain in the former.



**Fig. 12.** Effect of imidazole concentration on oxidation of cyclooctene by **2**. Reaction conditions: cyclooctene (1.0 mmol), *n*-octane (1.0 mmol), catalyst (0.0022 mmol), acetonitrile (5.0 ml), TBHP (2.0 mmol) and temperature ( $60 \pm 1$  °C).

**Table 6**  
Oxidation of various olefins catalyzed by **2**.

No.	Olefin	Product(s)	% Yield Time 4 h (24 h)	% Conversion Time 24 h
1			53 (80)	80
2			55 (70)	70
3			12 (47)	47
4			33 (60)	73
			– (8)	
			– (5)	
5			8 (15) <sup>a</sup>	31
6			– (9)	9
7	1-octene	1-octene oxide 2-octanone	4 (35) – (38)	73
8			– (60) <sup>b</sup>	60
9			– (63) <sup>b</sup>	63

Reaction conditions: olefin (1.0 mmol), TBHP (2 mmol), catalyst **2** (0.0022 mmol), acetonitrile (5 ml) and temperature (60 ± 1 °C). Conversions and yields are based on the starting substrate.

<sup>a</sup> The only *endo*-norbornene oxide product was confirmed by <sup>1</sup>H NMR, δ 3.4 ppm.

<sup>b</sup> Yields determined by <sup>1</sup>H NMR.

In the epoxidation of *cis*- and *trans*-stilbene the steric effects are distinct. The sterically demanding *trans*-stilbene is less reactive than the *cis* isomer. The oxygenation of *cis*-stilbene results in *trans*-stilbene oxide. Apparently, formation of the thermodynamically more stable *trans*-stilbene oxide requires a free rotation about the olefin C–C bond at some intermediate steps [36]; such a rotation is expected to be more feasible using catalysts with less steric strain. Typical epoxidizing reagents such as peroxyacids have been shown to react with *cis*-olefins about two times faster than the corresponding *trans*-olefin [37]. For *m*-chloroperoxybenzoic acid in methylene chloride at room temperature, *cis*- and *trans*-stilbenes are epoxidized at equal rates. This unequal reactivity was inferred to result from the nonbonded interactions between the phenyl groups of *trans*-stilbene and the aroylhydrazone ligand of the catalyst **2**.

Steric hindrance is also observed in the oxidation of indene and allylbenzene. Analyses of the reaction mixture of norbornene epoxidation with the system **2**/TBHP/Im/CH<sub>3</sub>CN by <sup>1</sup>H NMR in CHCl<sub>3</sub>-d displayed *endo*-norbornene oxide at 3.4 ppm (run no. 5, Table 6). The epoxidation of norbornene by *m*-chloroperbenzoic acid proceeds almost exclusively *exo* [38], whereas the formation of *exo*-norbornene oxide and *endo*-norbornene oxide in low

*exo/endo* ratio has been reported with iodosylarenes using several substituted tetraphenylporphyrin and tetrapyrrolylporphyrin iron(III) salts as catalysts [39]. A comparison of this catalytic system with previously reported systems shows that the conversion and the selectivity are higher than in the other systems [40].

#### 4. Conclusion

Our work has revealed that coordination complexes of Fe(III) and tridentate hydrazone Schiff base ligands obtained by reaction of benzhydrazide and 2-hydroxy-3-methoxybenzaldehyde derivatives afford a new class of Fe(III) catalysts for the oxidation of olefins.

Three Fe(III) complexes were prepared and it was demonstrated that these dissymmetric hydrazone Schiff base iron(III) complexes (**1–3**) are highly selective catalysts for the oxidation of various olefins by TBHP under mild conditions. The catalytic activity is further increased by the addition of imidazole. Electron-rich alkenes display higher reactivity than electron-poor ones. The potential of these catalysts in the oxidation of various olefins was proved by converting most of the investigated olefins to the corresponding epoxides by 100% selectivities. Both steric effects of the olefins and electronic effects of the catalyst ligands have an impact on the selectivity of the oxidation reactions.

#### Acknowledgments

We are grateful to the Zanjan University, the Faculty of Chemistry and Biochemistry of the Ludwig-Maximilians-Universität München, and the School of Chemistry for financial support of this study.

#### References

- [1] T. Młodnicka, B.R. James, in: F. Montanari, L. Casella (Eds.), *Metalloporphyrins Catalyzed Oxidations*, Kluwer, Dordrecht, the Netherlands, 1994, pp. 121–144.
- [2] R.A. Sheldon, in: B. Meunier (Ed.), *Biomimetic Oxidations Catalyzed by Transition Metal Complexes*, Imperial College Press, London, 2000.
- [3] M. Moghadam, V. Mirkhani, S. Tangestaninejad, I. Mohammdpour-Baltork, H. Kargar, *J. Mol. Catal. A: Chem.* 288 (2008) 116.
- [4] W. Zhang, J.L. Loebach, S.R. Wilson, E.N. Jacobsen, *J. Am. Chem. Soc.* 112 (1990) 2801.
- [5] R. Irie, K. Noda, Y. Ito, K. Katsuki, *Tetrahedron Lett.* 31 (1990) 7345.
- [6] O. Belda, C. Moberg, *Coord. Chem. Rev.* 249 (2005) 727.
- [7] Z. Xi, H. Wang, Y. Sun, N. Zhou, G. Cao, M. Li, *J. Mol. Catal. A: Chem.* 168 (2001) 299.
- [8] Z.H. Chohan, S.K.A. Sheazi, *Synth. React. Inorg. Met. Org. Chem.* 29 (1999) 105.
- [9] S. Goldstein, D. Meyerstein, *Acc. Chem. Res.* 32 (1999) 547.
- [10] M. Costas, K. Chen, L. Que Jr., *Coord. Chem. Rev.* 200–202 (2000) 517.
- [11] M. Costas, M.P. Mehn, M.P. Jensen, L. Que Jr., *Chem. Rev.* 104 (2004) 939.
- [12] E.Y. Tshuva, S.J. Lippard, *Chem. Rev.* 104 (2004) 987.
- [13] K.M. Kadish, K.M. Smith, R. Guilard (Eds.), *The Porphyrin Handbook*, Academic Press, San Diego, CA, 2000.
- [14] L. Savanini, L. Chiasserini, A. Gaeta, C. Pellerano, *Biorg. Med. Chem.* 10 (2002) 2193.
- [15] E. Ochiai, *Bioinorganic Chemistry*, Allyn and Bacon, Boston, 1977.
- [16] I.A. Tossadis, C.A. Bolos, P.N. Aslanidis, G.A. Katsoulos, *Inorg. Chim. Acta* 133 (1987) 275.
- [17] J.C. Craliz, J.C. Rub, D. Willis, J. Edger, *Nature* 34 (1955) 176.
- [18] J.R. Dilworth, *Coord. Chem. Rev.* 21 (1976) 29.
- [19] J.R. Merchant, D.S. Clothia, *J. Med. Chem.* 13 (1970) 335.
- [20] M.L. Vitolo, J. Webb, *J. Inorg. Biochem.* 20 (1984) 255.
- [21] E. Baker, M.L. Vitolo, J. Webb, *Biochim. Pharmacol.* 34 (1985) 3011.
- [22] P. Ponka, D. Richardson, E. Baker, H.M. Schulman, J.T. Edward, *Biochim. Biophys. Acta* 967 (1988) 122.
- [23] L. Pickart, W.H. Goodwin, W. Burgua, T.B. Murphy, D.K. Johnson, *Biochem. Pharmacol.* 32 (1983) 3868.
- [24] E.W. Ainscough, A.M. Brodie, A. Dobbs, J.D. Ranford, J.M. Waters, *Inorg. Chim. Acta* 267 (1998) 27.
- [25] M. El-Beheri, H. El-Twigry, *Spectrochim. Acta, Part A* 66 (2007) 28.
- [26] O. Pouralimardan, A.-C. Chamayou, C. Janiak, H. Hosseini-Monfared, *Inorg. Chim. Acta* 360 (2007) 360.
- [27] A. Altomare, M.C. Burla, M. Camalli, G.L. Cascarano, C. Giacovazzo, A. Guagliardi, A.G.G. Moliterni, G. Polidori, R. Spagna, *J. Appl. Crystallogr.* 32 (1999) 115.
- [28] G.M. Sheldrick, *SHELXS/L-97, Programs for Crystal Structure Determination*, University of Göttingen, Göttingen (Germany), 1997.

- [29] L.J. Farrugia, *J. Appl. Cryst.* 30 (1997) 565.
- [30] X.M. Zhang, *Coord. Chem. Rev.* 249 (2005) 1201.
- [31] H. Hosseini Monfared, Z. Kalantari, M.-A. Kamyabi, C. Janiak, *Z. Anorg. Allg. Chem.* 633 (2007) 1945.
- [32] M.-A. Kamyabi, S. Shahabi, H. Hosseini Monfared, *J. Chem. Eng. Data* 53 (2008) 2341.
- [33] C.K. Chang, T.G. Traylor, *J. Am. Chem. Soc.* 12 (1973) 8477.
- [34] D. Mohajer, H. Hosseini Monfared, *J. Chem. Res.* (1998) 772.
- [35] A.J. Appleton, S. Evans, J.R. Lindsay Smith, *J. Chem. Soc. Perkin Trans. 2* (1995) 281.
- [36] J.T. Groves, T.E. Nemo, *J. Am. Chem. Soc.* 105 (1983) 5786.
- [37] B.M. Lynch, K.H. Pausacker, *J. Chem. Soc.* (1955) 1525.
- [38] H.C. Brown, J.H. Kawakami, S. Ikegami, *J. Am. Chem. Soc.* 18 (1970) 2914.
- [39] D. Ostovic, T.C. Bruice, *Acc. Chem. Res.* 25 (1992) 314.
- [40] V. Mirkhani, M. Moghadam, S. Tangestaninejad, I. Mohammadpoor-Baltork, N. Rasouli, *Inorg. Chem. Commun.* 10 (2007) 1537.